Oligomerization of $Au(CN)_2^-$ and $Ag(CN)_2^-$ Ions in Solution via Ground-State Aurophilic and Argentophilic Bonding

Manal A. Rawashdeh-Omary,[†,‡] Mohammad A. Omary,[†,‡] and Howard H. Patterson*[,†]

Contribution from the Department of Chemistry, University of Maine, 5706 Aubert Hall, Orono, Maine 04469-5706

Received May 4, 2000

Abstract: Dicyanoaurate(I) and dicyanoargentate(I) ions undergo significant oligomerization in aqueous and methanolic solutions. The absorption edges of $K[Au(CN)_2]$ and $K[Ag(CN)_2]$ solutions undergo progressive red shifts with an increase in concentration up to near the saturation limits, whereupon total red shifts of 13.4 $\times$ 10^3 and 11.9 $\times$ 10^3 cm^{-1} are obtained from the respective maxima of the corresponding lowest energy monomer bands. Two types of deviations from Beer's law are observed: a negative deviation for the monomers' MLCT bands and a positive deviation for the oligomers' bands. Increasing the concentration within a given concentration range leads to red shifts in the oligomers' absorption and/or excitation bands dominant in that range, while further increases in concentration lead to the appearance of new lower energy bands. Electronic structure calculations suggest that this behavior is attributed to metal−metal interactions between neighboring $Au(CN)_2^-$ or $Ag(CN)_2^-$ ions. Formation constants of 1.50 $\pm$ 0.05 and 17.9 $\pm$ 2.0 M^{-1} are obtained for $[Ag(CN)_2^-]_2$ and $[Au(CN)_2^-]_2$ dimers, respectively, at ambient temperature.

Introduction

Dicyano complexes of Au(I) and Ag(I) have been known for a very long time. These complexes are among the most stable two-coordinate complexes of the transition metal ions, with stability constants of 10^{37} and 10^{20} M^{-2} for $Au(CN)_2^-$ and $Ag(CN)_2^-$, respectively.[1] Interest in these complexes has continued since the nineteenth century until today due to their importance in both science and applications.[1−3] Examples include the use of both the dicyanoaurates(I) and dicyanoargentates(I) in semiconductor materials,[3] the role of $Au(CN)_2^-$ in medical therapy after the intake of gold drugs for the treatment of rheumatoid arthritis,[2b] and in the carbon-in-pulp (CIP) process for gold extraction.[2c] A study of the association of the d^{10} $Au(CN)_2^-$ and $Ag(CN)_2^-$ ions is essential for understanding what is now called closed-shell interactions of the coinage metal cation complexes, as well as for understanding the role of these ions in some of their existing and potential applications. For example, it is now believed that one important aspect of the CIP process involves the association of $Au(CN)_2^-$ ions adsorbed on the carbon surface.

The molecular structure is similar for both $M[Au(CN)_2]$ and $M[Ag(CN)_2]$ solid salts, consisting of linear two-coordinate complex ions distributed in two-dimensional layers.[4−8] The M^+ ions bond directly to the cyanide ligands in the complex and/or to water molecules in hydrated compounds. Many examples have been reported in which stacked layers of $Au(CN)_2^-$ or $Ag(CN)_2^-$ alternate with layers of the counterion in a variety of fascinating two-dimensional topologies. Examples include the Kagomé net structure for $K[Au(CN)_2]$ and $K_2Na[Ag(CN)_2]$,[6,7] and the interpenetrating 6-connected nets of α-polonium type for $Rb[Cd\{[Ag(CN)_2]\}_3]$.[8] Several vibrational studies have been reported for $M[Au(CN)_2]$ and $M[Ag(CN)_2]$ compounds. These studies support the simple linear structures of the complex ions in both the solution and the solid state.[9−12] Metal−metal interactions are believed to be the reason for the formation of the stacked structures of $M[Au(CN)_2]$ and $M[Ag(CN)_2]$ compounds. Several studies have attributed the lower energies of the luminescence bands of $M[Au(CN)_2]$ and $M[Ag(CN)_2]$ solids to Au−Au and Ag−Ag interactions, respectively.[13−16]

† University of Maine.

‡ Present address: Department of Chemistry, Texas A&M University, College Station, TX 77843.

(1) Sharpe, A. G. *The Chemistry of Cyano Complexes of the Transition Metals*; Academic Press: London, 1976.

(2) (a) *Gold: Progress in Chemistry, Biochemistry and Technology*; Schmidbaur, H., Ed.; Wiley: Chichester, New York, 1999. (b) Shaw, C. F., III The Biochemistry of Gold. In *Gold: Progress in Chemistry, Biochemistry and Technology*; Schmidbaur, H., Ed.; Wiley: Chichester, New York, 1999; Chapter 10. (c) Adams, M. D.; Johns, M. W.; Dew, D. W. Recovery of Gold from Ores and Environmental Aspects. In *Gold: Progress in Chemistry, Biochemistry and Technology*; Schmidbaur, H., Ed.; Wiley: Chichester, New York, 1999; Chapter 3.

(3) (a) Kurmoo, M.; Day, P.; Mitani, T.; Kitagawa, H.; Shimoda, H.; Yoshida, D.; Guionneau, P.; Barrans, Y.; Chasseau, D.; Ducasse, L. *Bull. Chem. Soc. Jpn.* **1996**, *69*, 1233. (b) Chasseau, D.; Guionneau, P.; Rahal, M.; Bravic, G.; Gaultier, J.; Ducasse, L.; Kurmoo, M.; Day, P. *Synth. Met.* **1995**, *70*, 945. (c) Fujiwara, H.; Kobayashi, H. *Chem. Commun.* **1999**, *23*, 2417. (d) Kurmoo, M.; Pritchard, K. L.; Talham, D. R.; Day, P.; Stringer, A. M.; Howard, J. A. K. *Acta Crystallogr.* **1990**, *B46*, 348.

(4) (a) Blom, N.; Ludi, A.; Bürgi, H.-B.; Tichý, K. *Acta Crystallogr.* **1984**, *C40*, 1767. (b) Blom, N.; Ludi, A.; Bürgi, H.-B. *Acta Crystallogr.* **1984**, *C40*, 1770. (c) Range, K. J.; Kühnel, S.; Zabel, M. *Acta Crystallogr.* **1989**, *C45*, 1419. (d) Hoard, J. L. *Z. Kristallogr.* **1933**, *84*, 231. (e) Staritzky, E. *Anal. Chem.* **1956**, *28*, 419. (f) Range, K. J.; Zabel, M.; Meyer, H.; Fischer, H. *Z. Naturforsch.* **1985**, *40B*, 618. (g) Assefa, Z.; Staples, R.; Fackler, J. P., Jr.; Patterson, H. H.; Shankle, G. *Acta Crystallogr.* **1995**, *C51*, 2527. (h) Assefa, Z.; Shankle, G.; Patterson, H. H.; Reynolds, R. *Inorg. Chem.* **1994**, *33*, 2187.

(5) Omary, M. A.; Webb, T. R.; Assefa, Z.; Shankle, G. E.; Patterson, H. H. *Inorg. Chem.* **1998**, *37*, 1380.

(6) Rosenzweig, A.; Cromer, D. T. *Acta Crystallogr.* **1959**, *12*, 709.

(7) Zabel, M.; Kühnel, S.; Range, K. J. *Acta Crystallogr.* **1989**, *C45*, 1619.

(8) Hoskins, B. F.; Robson, R.; Scarlett, N. V. Y. *J. Chem. Soc., Chem. Commun.* **1994**, 2025.

(9) Chadwick, B. M.; Frankiss, S. G. *J. Mol. Struct.* **1976**, *31*, 281.

(10) Stammerich, H.; Chadwick, B. M.; Frankiss, S. G. *J. Mol. Struct.* **1967−68**, *1*, 191.

(11) Chadwick, B. M.; Frankiss, S. G. *J. Mol. Struct.* **1968**, *2*, 281.

(12) (a) Wong, P. T. T. *J. Chem. Phys.* **1979**, *70*, 456. (b) Bottger, G. L. *Spectrochim. Acta Part A* **1968**, *24*, 1821. (c) Loehr, T. M.; Long, T. V., II *J. Chem. Phys.* **1970**, *53*, 4182.

10.1021/ja001545w CCC: $19.00
Published on Web 10/04/2000

Dilute solutions of $Au(CN)_2^-$ and $Ag(CN)_2^-$ are dominated by monomers; thus, metal−metal interactions are expected to play little or no role in determining the electronic structure. Several studies have aimed at the characterization of the electronic structures of $Au(CN)_2^-$ and $Ag(CN)_2^-$ ions, most of which have been limited to absorption measurements of dilute aqueous solutions at ambient temperature.[17−22] Characterization of the electronic structure of linear dicyano complexes in general has been reported by Mason.[23] The electronic structure of $Au(CN)_2^-$ has been described in detail by interpreting the highly resolved absorption spectra of dilute $Au(CN)_2^-$ solutions[23] and thin films of solid $[(n\text{-}C_4H_9)_4N][Au(CN)_2]$ at cryogenic temperatures.[24] The strong absorption bands of $Au(CN)_2^-$ in the $40-54 \times 10^3$ cm^{-1} ultraviolet range have been assigned to individual spin−orbit states of a metal-to-ligand charge transfer (MLCT) nature.[23,24] The spectra of the corresponding Ag(I) compounds are less resolved; therefore, the assignment of the absorption bands of the $Ag(CN)_2^-$ monomer is less clear.[23] The effect of concentration on the absorption spectra of $Au(CN)_2^-$ and $Ag(CN)_2^-$ has not been addressed in Mason's work. To our knowledge, no luminescence studies have been reported for either $Au(CN)_2^-$ or $Ag(CN)_2^-$ in solution prior to the work described herein.

A fundamental issue that we are trying to address in our study of $Au(CN)_2^-$ and $Ag(CN)_2^-$ solutions is comparing Au−Au bonding versus Ag−Ag bonding in the ground and excited states. Ground-state Au−Au bonding interactions in coordination compounds of Au(I) have been studied extensively, both experimentally and theoretically.[2a] It is important to compare the extent and nature of Au−Au versus Ag−Ag bonding interactions based on structural, spectroscopic, and theoretical studies of similar Au(I) and Ag(I) compounds. Comparative structural studies are rare because, unfortunately, it is not easy to isolate compounds of the two metal ions with identical ligands, counterions, coordination number, geometry, and space group. One such study has been reported by Schmidbaur et al., who concluded that gold is slightly "smaller" than silver.[25] Extended one-dimensional chain structures of isomorphous complexes of Au(I) and Ag(I) with the same ligands have been reported by Fackler's group in two separate publications.[26,27] The intermolecular metal−metal distances in these chains are virtually identical (~3.22 Å) for both the Au(I) and Ag(I) complexes. Many investigations have addressed the issue of the relationship between the electronic properties of gold(I) compounds to the so-called *aurophilic attraction*,[28,29] and our group has recently reported similar studies for the analogous *argentophilic attraction*.[5,15,16,30] Recently, Che and co-workers have reported resonance Raman studies that confirm the bonding character of aurophilic and argentophilic interactions in binuclear complexes of Au(I) and Ag(I), respectively.[31,32] Systematic absorption and/or luminescence studies that compare Au−Au versus Ag−Ag bonding in similar complexes have been lacking until the present study. Nevertheless, structural and theoretical studies well establish that aurophilic bonds in monovalent coordination compounds are as strong as typical hydrogen bonds and that the corresponding Ag−Ag bonds are weaker. It is interesting given this fact to see whether such weak ground-state bonding leads to oligomerization in solution, a question that the present study answers. Excited-state interactions have been reported for Ag(I) systems.[15,30,33] For example, our group has reported excited-state Ag−Ag bonding interactions between adjacent $Ag(CN)_2^-$ ions in solid compounds, leading to the formation of Ag−Ag bonded excimers and exciplexes.[15,30] Recent results in our laboratory indicate that a similar phenomenon exists for $Au(CN)_2^-$ systems.[34] We address the question of excited-state interactions in solutions of $K[Au(CN)_2]$ and $K[Ag(CN)_2]$ in another paper.[35]

In this paper we study ground state aurophilic and argentophilic bonding both experimentally and theoretically. We report absorption and luminescence excitation spectra of $K[Au(CN)_2]$ and $K[Ag(CN)_2]$ in solution. The effects of concentration, temperature, and solvent on the absorption and excitation bands of $Au(CN)_2^-$ and $Ag(CN)_2^-$ are studied. Analysis is carried out for the effect of concentration on the absorption bands assigned to $Au(CN)_2^-$ and $Ag(CN)_2^-$ monomers as well as the appearance of new bands characteristic of oligomers. The temperature dependence of the electronic spectra is studied to see whether cooling enhances the oligomerization of $Au(CN)_2^-$ and $Ag(CN)_2^-$ ions at cryogenic temperatures. The solvent effect is also studied to compare the electronic structure of dicyanoaurates(I) and dicyanoargentates(I) in aqueous versus nonaqueous solvents. The fact that organic solvents such as methanol form transparent glasses at cryogenic temperatures[36] allows a better concentration-dependent luminescence study of frozen solutions in these

(13) (a) Fischer, P.; Mesot, J.; Lucas, B.; Ludi, A.; Patterson, H. H.; Hewat, A. *Inorg. Chem.* **1997**, *36*, 2791. (b) Fischer, P.; Ludi, A.; Patterson, H. H.; Hewat, A. W. *Inorg. Chem.* **1994**, *33*, 62. (c) Assefa, Z.; DeStefano, F.; Garepapaghi, M. A.; LaCasce, J. H., Jr.; Ouellette, S.; Corson, M. R.; Nagle, J. K.; Patterson, H. H. *Inorg. Chem.* **1991**, *30*, 2868. (d) Nagle, J. K.; LaCasce, J. H., Jr.; Dolan, P. J., Jr.; Corson, M. R.; Assefa, Z.; Patterson, H. H. *Mol. Cryst. Liq. Cryst.* **1990**, *181*, 359. (e) Nagasundaram, N.; Roper, G.; Biscoe, J.; Chai, J. W.; Patterson, H. H.; Blom, N.; Ludi, A. *Inorg. Chem.* **1986**, *25*, 2947. (f) Markert, J. T.; Blom, N.; Roper, G.; Perregaux, A. D.; Nagasundaram, N.; Corson, M. R.; Ludi, A.; Nagle, J. K.; Patterson, H. H. *Chem. Phys. Lett.* **1985**, *118*, 258. (g) Patterson, H. H.; Roper, G.; Biscoe, J.; Ludi, A.; Blom, N. *J. Lumin.* **1984**, *31/32*, 555.

(14) Yersin, H.; Riedl, U. *Inorg. Chem.* **1995**, *34*, 1642.

(15) Omary, M. A.; Patterson, H. H. *Inorg. Chem.* **1998**, *37*, 1060.

(16) Omary, M. A.; Patterson, H. H.; Shankle, G. *Mol. Cryst. Liq. Cryst.* **1996**, *284*, 399.

(17) Brigando, J. *Bull. Soc. Chim. Fr.* **1957**, *4*, 503.

(18) Simposon, E. A.; Waind, G. N. *J. Chem. Soc.* **1958**, 1748.

(19) (a) Jørgensen, C. K. *Adv. Chem. Phys.* **1963**, *5*, 33. (b) Jørgensen, C. K. *Absorption Spectra and Chemical Bonding in Complexes*; Pergamon Press: Oxford, 1962.

(20) Erny, M.; Lucas, R. C. R. *Acad. Sci., Ser. B* **1971**, *72*, 603.

(21) (a) Orgel, L. E. *J. Chem. Soc.* **1958**, 4186. (b) Dunitz, J.; Orgel, L. E. *Adv. Inorg. Chem. Radichem.* **1960**, *2*, 25.

(22) Perumareddi, J. R.; Liehr, A. D.; Adamson, A. W. *J. Am. Chem. Soc.* **1963**, *85*, 249.

(23) Mason, W. R. *J. Am. Chem. Soc.* **1973**, *95*, 3573.

(24) Mason, W. R. *J. Am. Chem. Soc.* **1976**, *98*, 5182.

(25) (a) Tripathi, U. M.; Bauer, A.; Schmidbaur, H. *J. Chem. Soc., Dalton Trans.* **1997**, 2865. (b) Bayler, A.; Schier, A.; Bowmaker, G. A.; Schmidbaur, H. *J. Am. Chem. Soc.* **1996**, *118*, 7006.

(26) Mazany, A. M.; Fackler, J. P., Jr. *J. Am. Chem. Soc.* **1984**, *106*, 801.

(27) Wang, S.; Fackler, J. P., Jr.; Carlson, T. F. *Organometallics* **1990**, *9*, 1973.

(28) Assefa, Z.; McBurnett, B. G.; Staples, R. J.; Fackler, J. P., Jr.; Assmann, B.; Angermaier, K.; Schmidbaur, H. *Inorg. Chem.* **1995**, *34*, 75.

(29) For recent reviews see: (a) Bowmaker, G. A. Spectroscopic Methods in Gold Chemistry. In *Gold: Progress in Chemistry, Biochemistry and Technology*; Schmidbaur, H., Ed.; Wiley: Chichester, New York, 1999; Chapter 21. (b) Forward, J. M.; Fackler, J. P., Jr.; Assefa, Z. Photophysical and Photochemical Properties of Gold(I) Complexes. In *Optoelectronic Properties of Inorganic Compounds*; Roundhill, D. M., Fackler, J. P., Jr., Eds.; Plenum Press: New York, 1999; Chapter 6.

(30) Omary, M. A.; Patterson, H. H. *J. Am. Chem. Soc.* **1998**, *120*, 7696.

(31) Leung, K. H.; Phillips, D. L.; Tse, M. C.; Che, C. M.; Miskowski, V. M. *J. Am. Chem. Soc.* **1999**, *121*, 4799.

(32) Che, C. M.; Tse, M. C.; Chan, M. C. W.; Cheung, K. K.; Phillips, D. L.; Leung, K. H. *J. Am. Chem. Soc.* **2000**, *122*, 2464.

(33) Henary, M.; Zink, J. I. *J. Am Chem. Soc.* **1989**, *111*, 7407.

(34) Rawashdeh-Omary, M. A. Ph.D. Thesis, Graduate School, University of Maine, 1999.

(35) Rawashdeh-Omary, M. A.; Omary, M. A.; Patterson, H. H. Photophysics of $[Au(CN)_2^-]_n$ and $[Ag(CN)_2^-]_n$ Oligomers in Solution. In preparation.

(36) Murov, S. L.; Carmichael, I.; Hug, G. L. *Handbook of Photochemistry*, 2nd ed.; Marcel Dekker: New York, 1993; pp 294−297.

solvents than in aqueous solutions. We also present a comparison between Au−Au versus Ag−Ag bonding through theoretical models and relate the findings to the experimental results. We are aware of only one prior study in which the oligomerization of Au(I) complexes is characterized in nonaqueous solutions.[37] To our knowledge, the present paper is the first spectroscopic study that characterizes the oligomerization of Ag(I) species in any solution and Au(I) species in aqueous solutions. We also present the first experimental evidence for the cooperativity of the argentophilic attraction.

Experimental Section

Solutions of $K[Ag(CN)_2]$ and $K[Au(CN)_2]$ in water and methanol were prepared by directly dissolving the pure solids. Solid $K[Ag(CN)_2]$ and $K[Au(CN)_2]$ (≥99.9% pure) were obtained from Alpha and stored under vacuum in desiccators containing Drierite prior to the preparation of solutions. UV−vis absorption spectra were recorded using a Model DU-640 Beckman spectrophotometer. Steady-state photoluminescence spectra were recorded with a Model QuantaMaster-1046 photoluminescence spectrophotometer from Photon Technology International, PTI. The instrument is equipped with two excitation monochromators and a 75 W xenon lamp. The excitation spectra were corrected for spectral variations in lamp intensity, by following the standard quantum counter method[38] that entails dividing the raw data by the excitation spectrum of rhodamine B (λ_{em} = 635 nm). Absorption and luminescence measurements at ambient temperatures were carried out for aqueous and methanolic solutions of $K[Ag(CN)_2]$ and $K[Au(CN)_2]$ in standard 1-cm quartz cuvettes. However, 1-mm quartz cuvettes were also used for absorption measurements of concentrated solutions to attenuate the strong absorbance. Low-temperature luminescence measurements were carried out using frozen solutions of $K[Ag(CN)_2]$ and $K[Au(CN)_2]$ in water and methanol. The solutions were placed in supracell quartz capillary tubes and inserted into a liquid nitrogen Dewar flask with a supracell quartz window. Measurements for pure solvents were carried out as a control. Extended Hückel calculations were carried out using the FORTICON8 program (QCMP011) with relativistic parameters.[39] The details of the calculation, including the parameters and interatomic distances used, were published elsewhere.[5,13c,30]

Results and Discussion

1. Spectroscopic Results for $K[Au(CN)_2]$ Solutions. The absorption spectra of $K[Au(CN)_2]$ have been recorded in water and in methanol. Figure 1 shows the absorption spectra of 1.00×10^{-4} M solutions at ambient temperature. The profile of the absorption spectrum and the extinction coefficient values for the $Au(CN)_2^-$ aqueous solution are very similar to the data in Mason's study.[23] Figure 1 indicates that the absorption spectrum of $Au(CN)_2^-$ in methanol is very similar to the absorption spectrum of the aqueous solution at the same concentration. The extinction coefficients of the $Au(CN)_2^-$ absorption bands are slightly lower in methanol than in water. The high values of the molar extinction coefficients of the $Au(CN)_2^-$ absorption bands (10^3−10^4 levels) are due to the strongly allowed MLCT nature of the transitions responsible for these bands.[23,24] The strong spin−orbit coupling in gold is illustrated in Figure 1 by the presence of intense bands that are assigned as electronic transitions to triplet excited states.

Aqueous solutions of $K[Au(CN)_2]$ exhibit photoluminescence at ambient temperature when their concentration is ∼0.01 M and higher. Absorption measurements have been conducted for these solutions to study the possible role of oligomerization on the luminescence behavior of dicyanoaurate(I) solutions. The concentration has been systematically increased above 0.01 M until the saturation limit is reached at about 0.76 M. Figure 2 shows the absorption spectra of selected $K[Au(CN)_2]$ aqueous solutions versus concentration at ambient temperature. Increasing the concentration up to 10^{-2} M levels results in a gradual increase in the relative intensity of the lower energy MLCT absorption bands ($^1\Pi_u$-1 and $^3\Pi_u$-1) relative to the higher energy bands, indicating different sensitivities to concentration for these two groups of bands. The absorption spectrum of the 1.0×10^{-2} M solution of $K[Au(CN)_2]$ shows a new shoulder in the 250−270 nm region. This lower energy shoulder becomes a well-defined peak as the concentration is increased further toward 0.10 M. Meanwhile, the MLCT peaks of the dilute solutions become less resolved at higher concentrations. The spectra of concentrated solutions (>0.1 M) show absorption edges with steep gradients. These solutions absorb nearly all UV radiation with wavelengths shorter than their absorption edges (until the instrument limit of 190 nm). As the concentration is progressively increased the absorption edge undergoes a corresponding red shift. Oligomerization of $Au(CN)_2^-$ in water is clearly illustrated in Figure 2 because if only monomeric species exist, only the intensity of the monomer bands (Figure 1) will increase with no red shift for the absorption edge. It is noted that the absorption region for a given solution covers the whole absorption region for solutions with lower concentrations. This indicates the presence of both $Au(CN)_2^-$ monomers and $[Au(CN)_2^-]_n$ oligomers at higher concentrations.

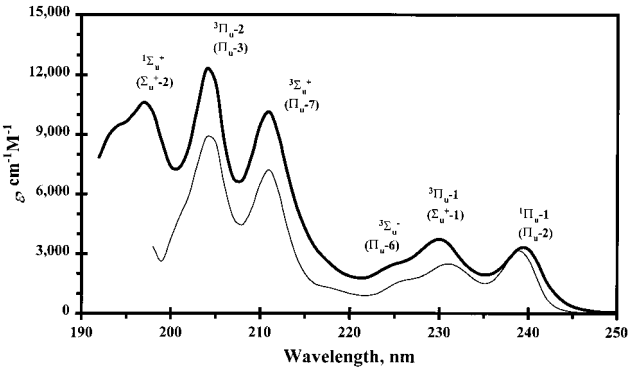

Figure 1. Absorption spectra of 1×10^{-4} M $K[Au(CN)_2]$ solutions in water (top) and methanol (bottom) at ambient temperature. The assignment is shown for each peak following the literature.[23,24] Spin−orbit states are shown in parentheses. Different electronic states that have the same designation are distinguished by the numbers after the dashes (e.g., the "2" in "Π_u-2" indicates that this is the second lowest energy Π_u state).

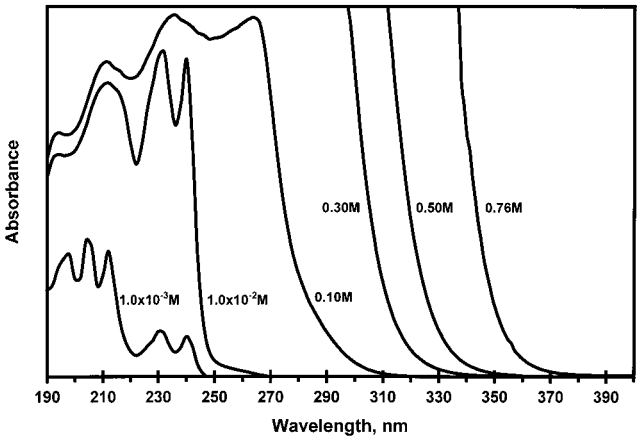

Figure 2. Absorption spectra versus concentration of $K[Au(CN)_2]$ in aqueous solutions at ambient temperature.

(37) Tang, S. S.; Chang, C. P.; Lin, I. J. B.; Liou, L. S.; Wang, J. C. *Inorg. Chem.* **1997**, *36*, 2294.
(38) Melhuish, W. H. *J. Opt. Soc. Am.* **1962**, *52*, 1256.
(39) Pyykkö, P.; Lohr, L. L. *Inorg. Chem.* **1981**, *20*, 1950.

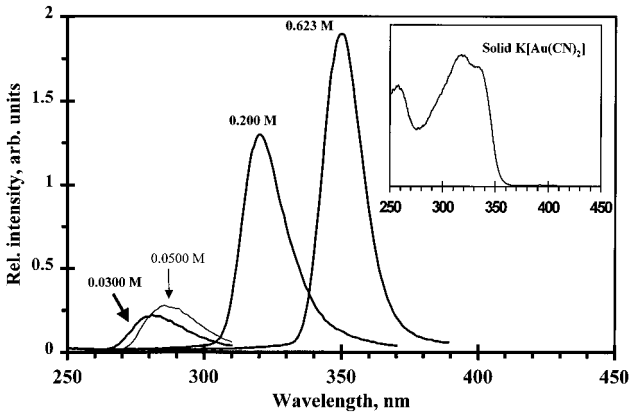

Figure 3. Corrected excitation spectra versus concentration of K[Au-$(CN)_2$] in aqueous solutions at ambient temperature. The inset shows the excitation spectrum of solid K[$Au(CN)_2$]. The emission is monitored at wavelengths that correspond to the maxima of the emission bands for each sample.

Because luminescence is inherently a more sensitive technique than absorption,[40] information about the oligomer transitions is better drawn from the luminescence excitation spectra than from the absorption spectra. Figure 3 shows the corrected excitation spectra of K[$Au(CN)_2$] aqueous solutions versus concentration at ambient temperature. It is striking to note that as the concentration increases, not only a red shift of one excitation band takes place, but also new lower energy bands appear. The appearance of well-resolved excitation bands for concentrated K[$Au(CN)_2$] aqueous solutions indicates the formation of different $[Au(CN)_2^-]_n$ oligomers in the ground state (i.e., dimers, trimers, tetramers, etc.). At a given concentration range at which a certain oligomer predominates, a relatively small increase in concentration leads to a red shift in the energy of the absorption band characteristic of that oligomer. This is illustrated in Figure 3 by the difference between the excitation spectra of the 0.0300 and 0.0500 M solutions. The excitation maxima for these two solutions appear at 281 and 286 nm, respectively. This is due to the reduction in the metal−metal distance in the oligomer responsible for this band upon increasing the concentration, leading to a smaller HOMO-LUMO energy gap, as it has been reported for Au(I)[28] and Ag(I)[15] complexes. If the concentration is increased an order of magnitude further, e.g. to 0.200 and 0.623 M, new excitation bands appear at 320 and 350 nm, respectively, due to the formation of new oligomers. The peak maximum at the saturation limit, represented by the 0.760 M solution, is 354 nm (not shown in Figure 3). The excitation peak of the saturated solution is red-shifted by ∼13 400 cm^{-1} from the lowest energy absorption peak of the monomer (Figure 1). This represents a very large shift and signifies ground-state Au−Au interactions in aqueous solutions of K[$Au(CN)_2$]. It is insightful to compare the oligomerization of the dicyanoaurates(I) in solution versus the solid state. The inset in Figure 3 shows the excitation spectrum of a single crystal of K[Au-$(CN)_2$] at ambient temperature. The excitation maximum for the solid appears at 332 nm. It is surprising that this wavelength is not only approached by a progressive increase in the concentration of aqueous solutions, but even exceeded in concentrated solutions. This surprising result may be due to the fact that the 2-dimensional layers of the $Au(CN)_2^-$ ions in the highly ordered crystals are separated by layers of the K^+ counterion,[6] whereas in solution the motion of the ions and water molecules is random and may allow for 3-dimensional interactions between $Au(CN)_2^-$ ions.

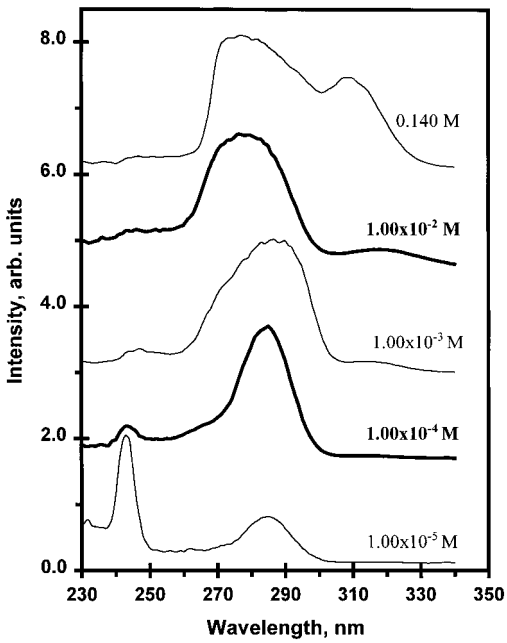

Figure 4. Corrected excitation spectra versus concentration of K[Au-$(CN)_2$] in methanol frozen solutions (77 K). The emission is monitored at 393 nm.

Solutions of K[$Au(CN)_2$] in methanol at ambient temperature show rather similar concentration dependence trends to those exhibited by aqueous solutions (see the Supporting Information). Therefore, oligomerization of $[Au(CN)_2^-]_n$ species in methanol occurs in a fashion similar to that in water. It was desired to study the oligomerization of $Au(CN)_2^-$ ions at low temperatures. Frozen solutions of K[$Au(CN)_2$] in methanol glasses exhibit strong luminescence with formal concentrations as low as 10^{-5} M.[41] Figure 4 shows the corrected excitation spectra of K[Au-$(CN)_2$] solutions in methanol at 77 K monitoring the emission at ∼390 nm. Figure 4 shows that the excitation spectrum of the lowest concentration solution studied (10^{-5} M) exhibits two peaks at 243 and 285 nm. The fact that the excitation peaks for this solution appear at much longer wavelengths than the absorption peaks of the same solution at ambient temperature underscores the oligomerization of $Au(CN)_2^-$ species at 77 K even at this extremely low concentration level. As the formal concentration of $Au(CN)_2^-$ in frozen methanol is increased to 10^{-4} M, the intensity of the longer wavelength peak increases relative to the shorter wavelength peak. A further increase in concentration to 10^{-3} M leads to the appearance of a new lower energy peak at ∼320 nm. The relative intensity of the 320-nm peak increases as the concentration is increased to 10^{-2} M. At the highest studied concentration of 0.14 M, the 320-nm peak becomes very pronounced while the 243-nm peak disappears. These results clearly illustrate the presence of at least three $[Au(CN)_2^-]_n$ oligomers in frozen solutions of K[$Au(CN)_2$] in methanol, and suggest the increasing tendency for the formation of the "larger" oligomers upon increasing the formal concentration. Thermal contraction of metal−metal distances upon cooling is responsible for the lower energies of the excitation bands at

(40) Skoog, D. A.; Holler, F. J.; Nieman, T. A. *Principles of Instrumental Analysis*, 5th ed.; Harcourt Brace: Philadelphia, 1998; Chapter 13.

(41) There are opposite trends for the volume change upon freezing aqueous versus methanolic solutions. While the volume of methanol decreases upon freezing, water expands. The concentration values in this work refer to the values at ambient temperature with no correction for volume changes upon cooling.

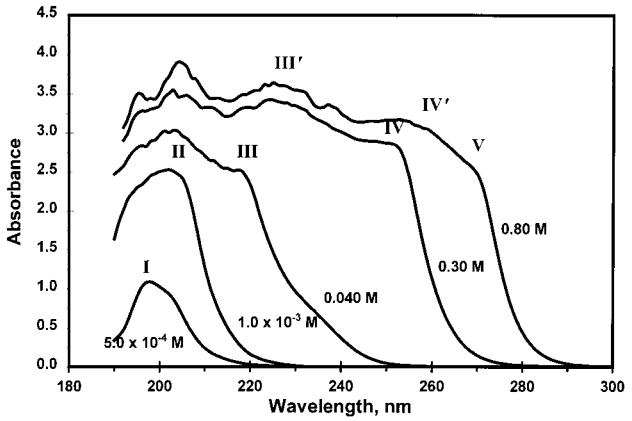

Figure 5. Absorption spectra versus concentration of $K[Ag(CN)_2]$ in aqueous solutions at ambient temperature.

cryogenic temperatures relative to ambient temperature, as it has been established for layered compounds of Au(I) and Ag(I).[13−16]

2. Spectroscopic Results for $K[Ag(CN)_2]$ Solutions. Figure 5 shows the absorption spectra of $K[Ag(CN)_2]$ aqueous solutions versus concentration at ambient temperature. The profile of the absorption spectrum for the 5.0×10^{-4} M $K[Ag(CN)_2]$ aqueous solution is very similar to the one reported by Mason.[23] The molar extinction coefficient (ϵ) value at the absorption maximum for this solution is about 21 700 $M^{-1}cm^{-1}$. The features labeled I and II in Figure 5 are assigned to monomer MLCT transitions from $^1\Sigma_g^+$ and $^1\Delta_g^+$ ground states to $^1\Pi_u$ excited states.[23] A major difference between the absorption spectra of dilute aqueous solutions of $K[Ag(CN)_2]$ and $K[Au(CN)_2]$ is the much lower resolution of the $Ag(CN)_2^-$ absorption bands. Figure 5 shows that the $Ag(CN)_2^-$ major absorption band in the dilute solution is not nearly as well-resolved as the highly structured $Au(CN)_2^-$ absorption bands (Figure 1). This result is a nice illustration of the effect of spin−orbit coupling on the absorption spectra. The spin−orbit coupling constant (ζ) is substantially higher for Au(I) than for Ag(I). The "ζ" value for the 5d orbital of Au(I) is 5100 cm^{-1}, compared with a corresponding value of 1830 cm^{-1} for the 4d orbital of Ag(I).[42] This results in much more splitting for the excited states of Au(I) versus Ag(I), as reflected by the difference in the structure of the monomer absorption bands between Figures 1 and 5.

The concentration dependence of the absorption spectra of aqueous solutions of $K[Ag(CN)_2]$ is qualitatively similar to that of $K[Au(CN)_2]$ solutions. The relative intensity of the lower energy monomer MLCT band II increases relative to feature I upon increasing the concentration, e.g. from 5.0×10^{-4} to 1.0×10^{-3} M. Further increases in concentration to 10^{-2} and 10^{-1} M levels lead to the progressive appearance of new longer wavelength features (see features III, IV, and V in Figure 5). In a concentration range at which one of these three features dominates, increasing the dicyanoargentate(I) concentration leads to a red shift for that feature (see III, III′; IV, IV′). The low-energy features in Figure 5 have a better resolution than that obtained for concentrated $K[Au(CN)_2]$ solutions, which allows a better quantitative analysis for concentrated $K[Ag(CN)_2]$ solutions (vide infra). Like the corresponding $K[Au(CN)_2]$ solutions, aqueous $K[Ag(CN)_2]$ solutions exhibit absorption edges with steep slopes that undergo progressive red shifts as concentration increases. The absorption edge for the 0.80 M solution (near the saturation limit) has an energy that is red-shifted by ∼11 900 cm^{-1} from the lowest energy absorption peak of the monomer (Figure 5). These results illustrate the oligomerization of $Ag(CN)_2^-$ anions in water. Similar results were obtained for $K[Ag(CN)_2]$ solutions in methanol (see the Supporting Information).

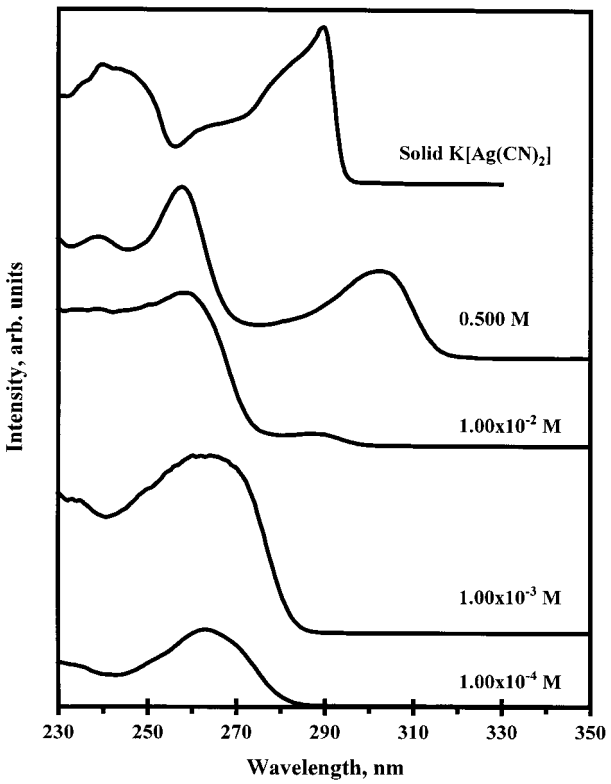

Figure 6. Corrected excitation spectra versus concentration of $K[Ag(CN)_2]$ in aqueous frozen solutions (77 K). The emission is monitored at 400 nm. The upper spectrum shows the excitation spectrum of solid $K[Ag(CN)_2]$ at 77 K.

Dicyanoargentate(I) solutions exhibit weak luminescence at ambient temperature and only at high concentrations. Therefore, low-temperature measurements are necessary to study the luminescence of $Ag(CN)_2^-$ species in aqueous solutions. We have carried out luminescence measurements for frozen solutions of $K[Ag(CN)_2]$ in both methanol and water. Here we summarize the results for frozen aqueous solutions. Frozen aqueous solutions exhibit strong luminescence with $Ag(CN)_2^-$ concentrations as low as 10^{-4} M. Figure 6 shows the corrected excitation spectra of frozen (77 K) aqueous solutions of $K[Ag(CN)_2]$ versus concentration. Two broad excitation bands appear with maxima near ∼250−260 and 290−305 nm, respectively. The relative intensity of the lower energy band increases with a progressive increase in the $Ag(CN)_2^-$ concentration. The maximum for the lower energy band of the 0.500 M solution is at even longer wavelength than that for a single crystal of $K[Ag(CN)_2]$ at 80 K. These results underscore the strong tendency for the oligomerization of $Ag(CN)_2^-$ species upon increasing the concentration. Frozen solutions of $K[Ag(CN)_2]$ in methanol showed similar results to those shown in Figure 6 (see the Supporting Information).

3. Non-Beer's Law Behavior of the Absorption Spectra. According to Beer's law, the profile of the absorption spectrum should be the same for solutions of the same analyte at different concentrations. Therefore, a plot of the extinction coefficient vs wavelength (or wavenumber) should be identical for solutions with different analyte concentrations if Beer's law is obeyed. Aqueous and methanolic solutions of $K[Ag(CN)_2]$ and K[Au-

(42) Griffith, J. S. *Theory of Transition Metal Ions*; Cambridge University Press: Cambridge, 1964.

Table 1. Deviation from Beer's Law for $K[Ag(CN)_2]$ and $K[Au(CN)_2]$ Aqueous Solutions (Extinction Coefficients for Each Type of Solution Are Listed at Two Wavelengths Representing Monomer and Dimer Bands, Respectively)[a]

$K[Ag(CN)_2]$ data			$K[Au(CN)_2]$ data		
c_0, M	ϵ_{197}, $M^{-1}\,cm^{-1}$	ϵ_{240}, $M^{-1}\,cm^{-1}$	c_0, M	ϵ_{204}, $M^{-1}\,cm^{-1}$	ϵ_{280}, $M^{-1}\,cm^{-1}$
1.00×10^{-6}	1.93×10^5		1.00×10^{-6}	3.26×10^5	
5.00×10^{-6}	7.16×10^4		5.00×10^{-6}	9.15×10^4	
5.00×10^{-5}	6.00×10^4		5.00×10^{-5}	4.57×10^4	
5.00×10^{-4}	2.15×10^4		5.00×10^{-4}	1.34×10^4	
5.00×10^{-3}	4.84×10^3		5.00×10^{-3}	6.08×10^3	
8.33×10^{-3}	3.01×10^3	30.9	2.00×10^{-2}	$(1.09 \times 10^3)^b$	2.01
1.67×10^{-2}	1.58×10^3	48.2	4.00×10^{-2}	$(762)^b$	20.8
3.33×10^{-2}	837	94.7	6.00×10^{-2}	*b*	32.5
5.55×10^{-2}	526	158	8.00×10^{-2}	*b*	49.6
6.66×10^{-2}	447	190	1.00×10^{-1}	*b*	65.1
8.33×10^{-2}	365	224	2.00×10^{-1}	*b*	141

[a] The extinction coefficient values are apparent ones, based on the given values of initial concentration (c_0). [b] These solutions are opaque at 204 nm. The ϵ values between parentheses are for the monomer band at 240 nm.

$(CN)_2]$ at ambient temperature show strong deviations from the Beer's law behavior. The molar extinction coefficients at maximum absorption, ϵ_{max}, are 1.93×10^5 and 3.26×10^5 M^{-1} cm^{-1} for 1.00×10^{-6} M aqueous solutions of $K[Ag(CN)_2]$ and $K[Au(CN)_2]$, respectively, at ambient temperature. These values are an order of magnitude greater than those reported by Mason.[23] The values of "ϵ_{max}" decrease orders of magnitude as the solute concentration is progressively increased. Table 1 summarizes the results for aqueous solutions. A similar behavior has been observed for methanolic solutions (some figures that pictorially illustrate the deviation from Beer's law for various solutions are deposited in the Supporting Information). These results, therefore, illustrate a strong negative deviation from Beer's law for the $K[Ag(CN)_2]$ aqueous solution. Real limitations to Beer's law are normally encountered when the analyte concentration is 0.01 M or higher.[40] The fact that the deviation from Beer's law occurs at much lower concentrations than 0.01 M for $K[Ag(CN)_2]$ and $K[Au(CN)_2]$ aqueous solutions suggests that this deviation is not due to real limitations to Beer's law. We attribute the deviation from Beer's law seen here to the oligomerization of the $Ag(CN)_2^-$ and $Au(CN)_2^-$ ions in solutions of $K[Ag(CN)_2]$ and $K[Au(CN)_2]$, respectively. Interestingly, when the concentration is high enough that new lower energy bands start to appear, an increase in concentration leads to a negative deviation from Beer's law for the higher energy bands accompanied by a positive deviation for the lower energy bands. The entries in the bottom part of Table 1 illustrate this behavior for aqueous solutions with concentrations in the 10^{-2} M level. The values are listed at two wavelengths for each compound, with the shorter wavelength representing a monomer band and the longer wavelength representing an oligomer band. Table 1 illustrates an unmistakable trend of negative deviation from Beer's law for monomer bands concomitant with a positive deviation for oligomer bands in both $K[Ag(CN)_2]$ and $K[Au(CN)_2]$.

The oligomerization process for $[M(CN)_2^-]$ (with M = Ag; Au) can be represented by eq 1, with an equilibrium constant given by eq 2:

$$n[M(CN)_2^-] \leftrightarrows [M(CN)_2^-]_n \quad (1)$$

$$K_{1n} = c_n/c_1^n \quad (2)$$

where c_1 and c_n refer to the concentrations of the monomer and the *n*-mer, respectively. If oligomerization indeed takes place as concentration increases, the "ϵ" values for the monomer bands will decrease while the "ϵ" values for the oligomer bands will increase, as illustrated indeed in Table 1.

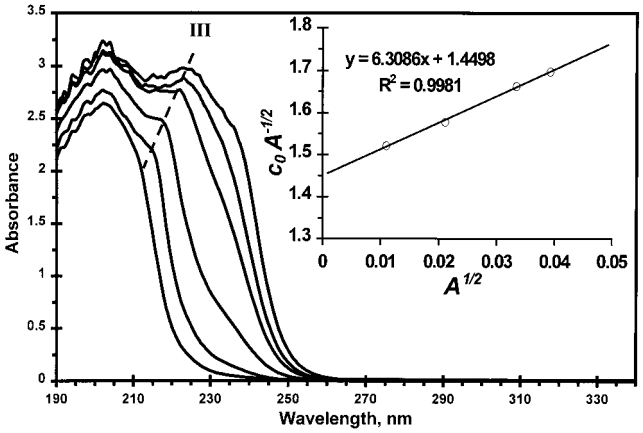

Figure 7. Absorption spectra versus concentration of $K[Ag(CN)_2]$ aqueous solutions at ambient temperature in the 10^{-2} M range. The inset shows a plot of $c_0A^{-1/2}$ vs $A^{1/2}$ with absorbance values taken at the band maxima for feature III, characteristic of a $[Ag(CN)_2^-]_2$ dimer.

When the initial $Ag(CN)_2^-$ concentration increases above certain values, the concentration of the $[Ag(CN)_2^-]_n$ oligomers may become high enough to observe new absorption bands at lower energies. Our results indicate the appearance of absorption features for more than one $[Ag(CN)_2^-]_n$ oligomer, each at a characteristic wavelength range over certain analyte concentrations (see the features labeled III, IV, and V in Figure 5). Figure 7 illustrates that feature III becomes more pronounced as the concentration is increased in the 10^{-2} M range. Features IV and V also appeared progressively as the concentration was increased to higher values (see the Supporting Information). We have carried out a quantitative analysis for the appearance of feature III as a function of the dicyanoargentate(I) concentration in the 10^{-2} M range. From Beer's law and eq 2, we can derive eq 3 by assuming that the appearance of feature III is due to the equilibrium shown in eq 1 (the derivation is in the Supporting Information):

$$c_0A^{-1/n} = (n/\{\epsilon_n b\})A^{(n-1)/n} + (K_{1n}\epsilon_n b)^{-1/n} \quad (3)$$

where c_0 is the initial dicyanoargentate(I) concentration (formality), A the maximum absorbance at feature III, ϵ_n the molar extinction coefficient of the *n*-mer, and b is the light path (0.1 cm). The inset in Figure 7 shows that a satisfactory fit was obtained by plotting $c_0A^{-1/2}$ vs $A^{1/2}$, thus suggesting that feature

Table 2. Summary of Extinction Coefficients, Formation Constants, and Free Energies for the Dicyanoargentate(I) and Dicyanoaurate(I) Oligomers in Aqueous Solutions of the Potassium Salts

species	ϵ, M^{-1} cm^{-1}	K	ΔG (295 K), kJ/mol
$[Ag(CN)_2^-]_2$	3.17 ± 0.10	1.50 ± 0.05 M^{-1}	-0.996 ± 0.075
$[Ag(CN)_2^-]_3$	13.3 ± 0.3	3.72 ± 0.09 M^{-2}	-3.22 ± 0.06
$[Au(CN)_2^-]_2$	3.94 ± 0.29	17.9 ± 2.0 M^{-1}	-7.08 ± 0.28

III is due to a $[Ag(CN)_2^-]_2$ dimer. From the equation of the straight line, a value of 1.50 ± 0.05 M^{-1} was derived for the formation constant of the dimer, K_{12}. It was desired to carry out a similar treatment for the determination of K_{13}, by assuming that feature IV (Figure 5) is due to a $[Ag(CN)_2^-]_3$ trimer. The absorption spectra for aqueous solutions of $K[Ag(CN)_2]$ show that feature IV becomes more pronounced when the initial concentration is increased in the 10^{-1} M level (e.g., see features IV and IV′ in Figure 5). One should note in Figure 5 that the appearance of feature IV is also accompanied by a strong absorption in the region of feature III. This suggests that $[Ag(CN)_2^-]_2$ dimers exist in solutions in which feature IV appears. Therefore, in the determination of K_{13} one should subtract the concentration of the dimer (using the derived value of K_{12}) from the initial dicyanoargentate(I) concentration. Using the corrected c_0 values, a plot of $c_0A^{-1/3}$ vs $A^{2/3}$ was linear ($R^2 = 0.9988$), suggesting trimer formation characteristic of feature IV (see the Supporting Information). From the equation of the straight line, a K_{13} value of 3.72 ± 0.09 M^{-2} was obtained. The positive deviation from Beer's law illustrated in Figure 7 for concentrated aqueous solutions of $K[Ag(CN)_2]$ is also evident in methanol solutions as well as in aqueous and methanol solutions of $K[Au(CN)_2]$. Analysis of the absorption data for $K[Au(CN)_2]$ solutions ($c_0 = 0.04-0.10$ M) leads to a K_{12} value of 17.9 ± 2.0 M^{-1} for $K[Au(CN)_2]$ (see the Supporting Information). The absorption maxima for more concentrated $K[Au(CN)_2]$ solutions exceeded the limits of the 1-mm cell we used, therefore a quantitative analysis to estimate K_{13} was not possible. Table 2 summarizes the results for the determination of formation constants, extinction coefficients, and free energies for $[Ag(CN)_2^-]_n$ and $[Au(CN)_2^-]_n$ oligomers in aqueous solutions.

Deviations from Beer's law have been reported for d^{10} and d^8 systems. We are aware of only one study prior to the work herein, by Schindler et al.,[43] in which a negative deviation from Beer's law is observed for the monomer MLCT bands in aqueous solutions of $Pt(CN)_4^{2-}$ (similar to the trend shown in Table 1). These authors have attributed the reduction in the "ϵ" values of the MLCT bands of $Pt(CN)_4^{2-}$ to the formation of oligomers (trimers). On the other hand, positive deviations from Beer's law have been reported for aqueous tetracyanoplatinates-(II)[43,44] and for acetonitrile solutions of dinuclear Au(I) compounds with diphosphine-dithiolate ligands.[37] To our knowledge, no concentration-dependent studies have been previously reported to characterize intermolecular interactions in Ag(I) systems. The formation constants for the Ag(I) oligomers (Table 2) are similar in magnitude to those reported by Lechner and Gliemann for the tetracyanoplatinates(II).[44] The formation constant and the corresponding ΔG value for $[Au(CN)_2^-]_2$ are clearly higher than those for $[Ag(CN)_2^-]_2$, as expected due to the stronger Au−Au bonds (vide infra). The ΔG value of -7.08 ± 0.28 kJ/mol for $[Au(CN)_2^-]_2$ at ambient temperature is slightly lower but similar in magnitude to the values reported by Lin and co-workers for dinuclear Au(I) compounds in acetonitrile solutions ($-\Delta G = 8.9-12.1$ kJ/mol).[37]

4. Electronic Structure Calculations. The optical results in the present study provide multiple evidence of significant oligomerization for both $Au(CN)_2^-$ and $Ag(CN)_2^-$ ions in solution. Negative deviation from Beer's law for the MLCT bands due to oligomerization occurs even at micromolar concentration levels. These results are surprising given the closed-shell nature of Au(I) and Ag(I) ions. Electronic structure calculations have been carried out to rationalize the optical results. The underlying goals of the calculations are several: first, to prove that oligomerization leads to significant reductions in HOMO-LUMO gaps and that these reductions are similar in magnitude to the experimental red shifts in the absorption energies upon increasing the concentration; second, to establish that oligomerization is a thermodynamically favorable process for both the dicyanoaurates(I) and dicyanoargentates(I); and third, to compare between aurophilic bonding and argentophilic bonding and relate the findings to the experimental results. Achieving these goals using ab initio or density functional methods requires a very long computation time because we are dealing with large oligomers of complexes of rather heavy atoms, the modeling of which requires an extremely large number of basis functions. Instead, we have pursued these goals using extended Hückel calculations with relativistic parameters.[39] Therefore, in the discussion of the results of these calculations we will be focusing on the differences between the calculation results for the models used, as opposed to the absolute energies and bond distances for individual models.

4.1. Oligomer Band Gaps. Aggregation of $Au(CN)_2^-$ and $Ag(CN)_2^-$ ions can be either one-dimensional (1-D) or two-dimensional (2-D). We have modeled 1-D and 2-D aggregations for both $Au(CN)_2^-$ and $Ag(CN)_2^-$. Figure 8a illustrates the effect of 1-D aggregation on the HOMO-LUMO gap for a homologous series of linear $[Ag(CN)_2^-]_n$ ions ($n = 1-7$; eclipsed conformers).[45] A progressive reduction in the HOMO-LUMO gap is observed upon increasing the oligomer size (n) and the orbital energies nearly converge at $n = 7$. According to Figure 8a, the reduction in the band gap is due to concomitant destabilization of the HOMO's and stabilization of the LUMO's. The Ag−Ag antibonding character is responsible for the destabilization of the HOMO's, while the Ag−Ag bonding character is responsible for the stabilization of the LUMO's.[15,30] Electronic structure calculations for linear $[Au(CN)_2^-]_n$ ions gave similar qualitative results as those shown in Figure 8a for $[Ag(CN)_2^-]_n$ ions.[34] The total reduction in the HOMO-LUMO gap from $n = 1$ to 7 is 1.33 eV for $[Ag(CN)_2^-]_n$ ions. This value corresponds to $\sim$11 000 cm^{-1}, which is similar to the magnitudes of the red shifts in the absorption edge of $K[Ag(CN)_2]$ solutions (inferred from Figure 5).

Figure 8b illustrates the effect of 2-D aggregation on the HOMO-LUMO gaps for $[Au(CN)_2^-]_n$ ions ($n = 1-5$).[45] A progressive reduction in the HOMO-LUMO gap is observed upon aggregation in the manner shown in Figure 8b. Similar to the trend in the 1-D aggregation, the reduction in the band gap due to 2-D aggregation is a result of concomitant destabilization of the HOMO's and stabilization of the LUMO's. Similar trends were obtained for 2-D aggregation of $[Ag(CN)_2^-]_n$ ions.[5,15,16,30]

(43) Schindler, J. W.; Fukuda, R. C.; Adamson, A. W. *J. Am. Chem. Soc.* **1982**, *104*, 3596.

(44) Gliemann, G.; Lechner, A. *J. Am. Chem. Soc.* **1989**, *111*, 7469.

(45) The geometry of the metal atoms and the dihedral angle of the cyanide ligands will lead to numerous isomers of the same $[M(CN)_2^-]_n$ oligomer (e.g., trimers may be either linear or angular; tetramers may be linear, zigzag, trapezoid, parallelogram, and square). Each isomer has a different absorption energy from the others (e.g., staggered isomers have lower energies than eclipsed ones of the same oligomer; linear trimers have lower energies than angular ones: see refs 30 and 62 for details).

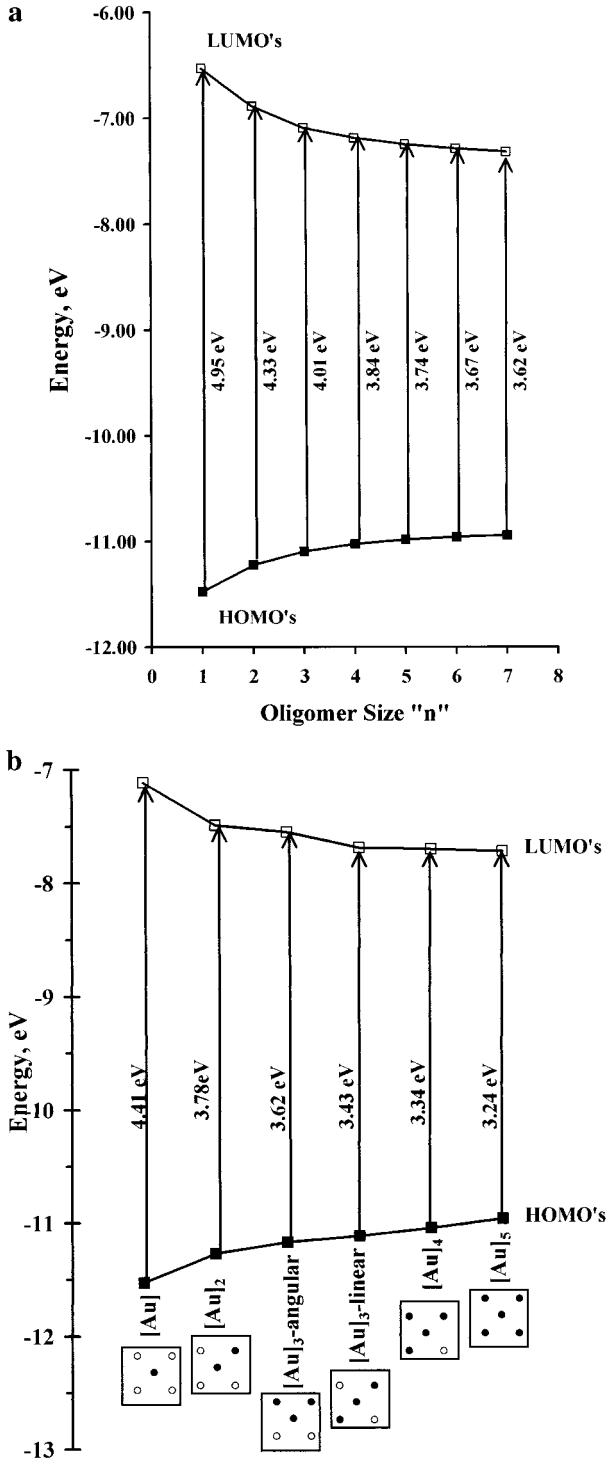

Figure 8. Energies of the highest occupied molecular orbital, HOMO, and the lowest unoccupied molecular orbital, LUMO, for (a) $[Ag(CN)_2^-]_n$ oligomers with $n = 1-7$ in a 1-dimensional array and (b) $[Au(CN)_2^-]_n$ oligomers with $n = 1-5$ in a 2-dimensional array. Energies are obtained by relativistic extended Hückel calculations for oligomers with eclipsed configurations.

The total reduction in the HOMO-LUMO gap as a result of 2-D aggregation of $[Au(CN)_2^-]_n$ ions is 1.17 eV. This value corresponds to ~9500 cm^{-1}, which is similar to the magnitudes of the red shifts in the absorption edge of $K[Au(CN)_2]$ solutions (inferred from Figure 2).

The absorption energies for saturated solutions and solid-state compounds of both $Au(CN)_2^-$ and $Ag(CN)_2^-$ are shifted from the monomer absorption peaks by even higher magnitudes

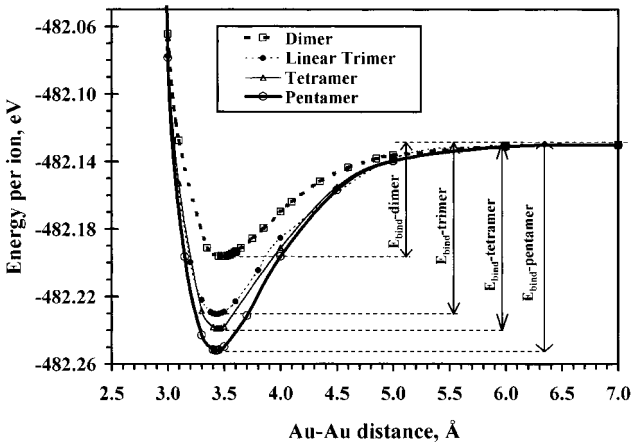

Figure 9. Potential energy diagrams for $[Au(CN)_2^-]_n$ oligomers with $n = 2-5$. Energies are obtained by relativistic extended Hückel calculations for oligomers with eclipsed configurations. The arrows show the binding energies (E_{bind}), which increase upon increasing "*n*".

than those predicted by the above calculations. According to the crystal structures of $M[Au(CN)_2]$ and $M[Ag(CN)_2]$ compounds, adjacent complex ions are distributed in two-dimensional layers with relatively short Au−Au and Ag−Ag distances.[2−8] Therefore, the 2-D model presented in Figure 8b provides a lower limit for the actual aggregation in solids and saturated solutions. The model in Figure 8b represents the first 2-dimensional shell of a given $Au(CN)_2^-$ (or $Ag(CN)_2^-$) ion. Further reduction in the HOMO-LUMO gap toward convergence will likely occur if one considers additional 2-dimensional shells.

4.2. Thermodynamic Tendency for Oligomerization. Extended Hückel calculations have been carried out for $[Au(CN)_2^-]_2$, $[Au(CN)_2^-]_3$, $[Au(CN)_2^-]_4$, and $[Au(CN)_2^-]_5$ isolated oligomers with different geometrical isomers. The potential energy diagrams for all these $[Au(CN)_2^-]_n$ oligomers have well minima, suggesting Au−Au bonding interactions. To illustrate the results, Figure 9 shows potential energy diagrams for $[Au(CN)_2^-]_n$ oligomers ($n = 2-5$; eclipsed isomers). According to Figure 9, the binding energy (depth of the potential well) for a $[Au(CN)_2^-]_n$ oligomer increases as "*n*" increases between 2 and 5. Similar trends have been obtained for the analogous Ag(I) oligomers.[5,30] Table 3 summarizes the results.[45]

The data in Table 3 indicate that the larger the number of monomer units "*n*" in the oligomer the higher the binding energy and the lower the electron energy per ion. This occurs despite the fact that the steric hindrance increases as "*n*" increases in these eclipsed oligomers. Thus, the stabilization due to gold−gold and silver−silver bonding is more important than the destabilization due to the steric hindrance. Therefore, these results suggest the presence of a thermodynamic driving force for the oligomerization of both the dicyanoaurates(I) and the dicyanoargentates(I). This conclusion is in agreement with the literature, in which numerous examples of cluster formation in compounds of Au(I)[2a,46−48] and Ag(I)[2−8,49−54] have been reported.

(46) Schmidbaur, H. *Chem. Soc. Rev.* **1995**, 391.
(47) Pyykkö, P. *Chem. Rev.* **1997**, *97*, 599.
(48) Balzani, V.; Scandola, F. *Supramolecular Photochemistry*; Ellis Horwood: Chichester, UK, 1991.
(49) Singh, K.; Long, J. R.; Stavropoulos, P. *J. Am. Chem. Soc.* **1997**, *119*, 2942.
(50) Fortin, D.; Drouin, M.; Turcotte, M.; Harvey, P. D. *J. Am. Chem. Soc.* **1997**, *119*, 531.
(51) (a) Linke, C.; Jansen, M. *Inorg. Chem.* **1994**, *33*, 2614. (b) Jansen, M.; Linke, C. *Angew. Chem.* **1992**, *104*, 618; *Angew. Chem., Int. Ed. Engl.* **1992**, *31*, 653.

Table 3. Summary of the Results of Ground-State Extended Hückel Calculations for $[Au(CN)_2^-]_n$ and $[Ag(CN)_2^-]_n$ Homologous Series (All Isomers Have an Eclipsed Geometry)[a]

model	[Au]	$[Au]_2$	$[Au]_3$ ang	$[Au]_3$ lin	$[Au]_4$	$[Au]_5$	[Ag]	$[Ag]_2$	$[Ag]_3$ ang	$[Ag]_3$ lin	$[Ag]_5$
M−M eq dist		3.48	3.48	3.44	3.44	3.43		3.55	3.54	3.49	3.44
bind E, eV	0	0.132	0.266	0.301	0.435	0.608	0	0.135	0.29	0.33	0.725
tot *E*, eV	−482.13	−964.39	−1446.66	−1446.69	−1928.96	−2411.26	−497.61	−995.35	−1493.12	−1493.16	−2491.63
E per ion	−482.13	−482.20	−482.22	−482.23	−482.24	−482.25	−497.61	−497.68	−497.71	−497.72	−498.33

[a] Notation: [Au], $[Au(CN)_2^-]$; [Ag], $[Ag(CN)_2^-]$; ang, angular (C_{2v}); lin, linear (D_{2h}); M, metal (Au; Ag); eq dist, equilibrium distance; bind *E*, binding energy; tot *E*, total one-electron energy.

Table 4. Comparison between Gold−Gold Interactions versus Silver−Silver Interactions Based on Extended Hückel Calculations for Staggered Models of $X[M(CN)_2^-]_2$ and $[M(CN)_2^-]_3$ (M = Au, Ag)

model	binding energy, eV	M−M bond energy, eV	M−M bond energy, kJ/mol
$[Au(CN)_2^-]_2$	0.298	0.298	28.8
$[Ag(CN)_2^-]_2$	0.218	0.218	21.0
$[Au(CN)_2^-]_3$	0.707	0.353	34.1
$[Ag(CN)_2^-]_3$	0.612	0.306	29.5

4.3. Gold−Gold Interactions versus Silver−Silver Interactions. Dicyanoaurate(I) and dicyanoargentate(I) oligomer ions are good models to study Au−Au and Ag−Ag interactions because the metal−metal bonding in these species is inherent and not ligand-assisted. A comparison of Au−Au versus Ag−Ag interactions in $[Au(CN)_2^-]_n$ and $[Ag(CN)_2^-]_n$ models of the same configuration is presented here. Metal−metal bonding is compared in staggered isomers to minimize steric contributions to the total energy. Table 4 provides a summary of extended Hückel calculations for staggered $[M(CN)_2^-]_2$ and $[M(CN)_2^-]_3$ (M = Au, Ag).

The calculated binding energies for $[Au(CN)_2^-]_2$ and $[Au(CN)_2^-]_3$ are 0.298 and 0.707 eV, respectively. That is, the Au−Au bond energy is ∼0.30−0.35 eV according to our calculations. This energy is in good agreement with the reported values of 0.2−0.5 eV based on many experimental and theoretical investigations for a variety of Au(I) compounds.[47,55−57] The results of the ground-state calculations show that Au(I) species give rise to stronger M−M bonding than the corresponding Ag(I) species. Table 4 shows that the Au−Au bond energy is stronger than the Ag−Ag bond by 7.8 and 4.6 kJ/mol in the ground-state dimer and trimer, respectively. The average ground-state Au−Au and Ag−Ag bond energies are 31.5 and 25.3 kJ/mol, respectively. While the value of the Au−Au binding energy is in excellent agreement with the reported values (average ∼34 kJ/mol),[47,55−57] to our knowledge no quantitative data are available in the literature for the ground-state Ag−Ag bond energy. The stronger ground-state bonding in Au(I) species is likely due to the relativistic effects, which are much stronger in gold than in silver. Pyykkö has attributed ∼20% of the Au−Au bonding energy in the ground state to the relativistic effects.[47] It is interesting to note that Table 4 indicates an average of ∼25% stronger Au−Au bonding than Ag−Ag bonding in the ground state.

Two theoretical models have been proposed in the literature to describe the rationale for ground-state Au(I)−Au(I) interactions. The first model, suggested by Hoffmann and co-workers, attributes Au−Au interactions to the hybridization of 5d orbitals with 6s and 6p orbitals.[58] The second model, suggested by Pyykkö and co-workers, attributes Au−Au interactions to correlation effects strengthened by relativistic effects.[59] Our group has reported electronic structure calculations for $Au(CN)_2^-$ and $Ag(CN)_2^-$ models. For the $Au(CN)_2^-$ ion, substituting relativistic parameters for nonrelativistic parameters has led to an increase in the Au contribution of the HOMO from 50% to 72% (22% 6s; 49% $5d_{z^2}$).[13c] Similar calculations for $Ag(CN)_2^-$ have shown 33% Ag character (16% 5s and 17% $4d_{z^2}$) in the HOMO with relativistic parameters.[16] These results illustrate the significant mixing between the $(n+1)$s with the *n*d orbitals for both $Au(CN)_2^-$ and $Ag(CN)_2^-$, in agreement with Hoffmann's model. Ground-state bonding between $Au(CN)_2^-$ ions is expected to be higher than that between $Ag(CN)_2^-$ ions due to the greater Au contribution in the HOMO as a result of the much stronger relativistic effects in gold compared to silver, in agreement with Pyykkö's model.

Concluding Remarks

This study provides multiple evidence for the oligomerization of $Au(CN)_2^-$ and $Ag(CN)_2^-$ ions in aqueous and methanolic solutions. Oligomerization results in a perturbation of the frontier molecular orbitals that are responsible for the optical transitions. The experimental and theoretical results both suggest the existence of ground-state Ag−Ag and Au−Au bonding interactions with the bonding slightly stronger for Au(I) than for Ag(I). Aqueous solutions of $K[Au(CN)_2]$ and $K[Ag(CN)_2]$ near the saturation limit have absorption edges that are red shifted by 13.4×10^3 and 11.9×10^3 cm^{-1}, respectively, relative to the absorption maxima of the corresponding lowest energy monomer bands. That is, the total red shift is 13% more for $K[Au(CN)_2]$ solutions. Hence, one would predict that the oligomerization of $Au(CN)_2^-$ ions leads to about 13% more reduction in the HOMO-LUMO gap than the case for $Ag(CN)_2^-$ ions. Extended Hückel calculations show that as one proceeds from monomers to staggered trimers,[60] the HOMO-LUMO gaps are lowered by 1.45 and 1.22 eV (11.7 and 9.84×10^3 cm^{-1}) for $Au(CN)_2^-$ and $Ag(CN)_2^-$ species, respectively. This represents 19% more stabilization for $Au(CN)_2^-$ species, in a

(52) Eastland, G. W.; Mazid, M. A.; Russell, D. R.; Symons, M. C. R. *J. Chem. Soc., Dalton Trans.* **1980**, 1682.
(53) (a) Kim, Y.; Seff, K. *J. Am. Chem. Soc.* **1977**, *99*, 7055. (b) Kim, Y.; Seff, K. *J. Am. Chem. Soc.* **1978**, *100*, 175.
(54) For a review see: Jansen, M. *Angew. Chem.* **1987**, *99*, 1136; *Angew. Chem., Int. Ed. Engl.* **1987**, *26*, 1098.
(55) (a) Jones, W. B.; Yuan, J.; Narayanaswamy, R.; Young, M. A.; Elder, R. C.; Bruce, A. E.; Bruce, M. R. M. *Inorg. Chem.* **1995**, *34*, 1996. (b) Narayanaswamy, R.; Young, M. A.; Parkhurst, E.; Ouellette, M.; Kerr, M. E.; Ho, D. M.; Elder, R. C.; Bruce, A. E.; Bruce, M. R. M. *Inorg. Chem.* **1993**, *32*, 2506.
(56) Harwell, D. E.; Mortimer, M. D.; Knobler, C. B.; Anet, F. A. L.; Hawthorne, M. F. *J. Am. Chem. Soc.* **1996**, *118*, 2679.
(57) (a) Zank, J.; Schier, A.; Schmidbaur, H. *J. Chem. Soc., Dalton Trans.* **1998**, 323. (b) Schmidbaur, H.; Graf, W.; Müller, G. *Angew. Chem., Int. Ed. Engl.* **1988**, *27*, 417.
(58) (a) Merz, K. M., Jr.; Hoffmann, R. *Inorg. Chem.* **1988**, *27*, 2120. (b) Jiang, Y.; Alvarez, S.; Hoffmann, R. *Inorg. Chem.* **1985**, *24*, 749. (c) Mehrotra, P. K.; Hoffmann, R. *Inorg. Chem.* **1978**, *17*, 2187. (d) Dedieu, A.; Hoffmann, R. *J. Am. Chem. Soc.* **1978**, *100*, 2074.
(59) (a) Klinkhammer, K. W.; Pyykkö, P. *Inorg. Chem.* **1995**, *34*, 4134. (b) Li, J.; Pyykkö, P. *Inorg. Chem.* **1993**, *32*, 2630. (c) Pyykkö, P.; Zhao, Y. F. *Angew. Chem.* **1991**, *103*, 622; *Angew. Chem., Int. Ed. Engl.* **1991**, *30*, 604. (d) Pyykkö, P.; Li, J.; Runeberg, N. *Chem. Phys. Lett.* **1994**, *218*, 133. (e) Li, J.; Pyykkö, P. *Chem. Phys. Lett.* **1992**, *197*, 586. (f) Pyykkö, P.; Zhao, Y. F. *Chem. Phys. Lett.* **1991**, *177*, 103.

reasonable agreement with the experimental value of 13% based on the absorption spectra.

The experimental and theoretical results in this work both predict that the oligomerization of $M(CN)_2^-$ ions (M = Au; Ag) is a cooperative process. The experimental results illustrate the cooperativity of the oligomerization process for $Ag(CN)_2^-$ ions. Table 2 shows that the ΔG value for $[Ag(CN)_2^-]_3$ (two Ag−Ag bonds) is more than twice the value for $[Ag(CN)_2^-]_2$ (one Ag−Ag bond) by ∼60%. We are not aware of any precedent to this study in the literature of d^{10} or d^8 coordination compounds, in which K or ΔG values were determined experimentally for more than one oligomer of the same monomer. The theoretical evidence for cooperativity is illustrated in Table 4, which clearly shows higher M−M bond energies in trimers than in dimers. The calculated M−M bond energies are 18 and 40% higher in the trimers than in the dimers for M = Au and Ag, respectively. Moreover, Table 3 shows that the total electronic energy per $M(CN)_2^-$ ion increases on oligomerization. That is, both the experiment and theory suggest significant cooperativity for the oligomerization of $Ag(CN)_2^-$ ions. Unfortunately, the strong absorbance of concentrated solutions of $K[Au(CN)_2]$ did not allow us to detect distinct peaks for $[Au(CN)_2^-]_3$ trimers to calculate the ΔG value for $[Au(CN)_2^-]_3$ and compare it with the value for $[Au(CN)_2^-]_2$. Nevertheless, the theoretical evidence based on Tables 3 and 4 clearly illustrates the cooperative nature of the oligomerization of both Au(I) and Ag(I) species. The greater thermodynamic stability for trimers versus dimers is also supported by structural studies, which have shown that several mononuclear compounds of Au(I)[61] and Ag(I)[5] appear as trimers in the solid state.

The strong dependence of the extinction coefficients on the "chromophore" concentration starts even at micromolar concentration values. Indeed, we propose, based on the drastic changes in the absorption and excitation spectra with concentration (Figures 2−6; Table 1), that solutions at different concentrations of $K[Ag(CN)_2]$ or $K[Au(CN)_2]$ actually represent "different chromophores". For example, the spectra shown in Figure 5 should be viewed as the spectra of five different chromophores, as opposed to the same chromophore with different concentrations, because each solution has a completely different absorption profile from the other. While this is an unusual trend, it is not unprecedented in the chemistry of Au(I) and Ag(I) compounds. For example, Jansen et al. have reported several studies that demonstrate that Ag(I) species in one material can exist in multiple cluster sites that have independent physical and chemical properties.[51,54] Furthermore, $Au(CN)_2^-$ and $Ag(CN)_2^-$ ions doped in alkali halide crystals show drastically different photophysical behavior for dimers versus trimers.[30,34,62,63] For example, the excitation and emission peaks for the dimers have been resolved from the trimer peaks by site-selective excitation;[30,63] and energy transfer pathways between dimers and trimers have been characterized both qualitatively and quantitatively by time-resolved luminescence spectroscopy.[62]

Acknowledgment. The authors thank the donors of the Petroleum Research Fund, administered by the American Chemical Society, for their support of this research.

Supporting Information Available: Derivation of the equations used for quantitative analysis and additional absorption and excitation data and spectral analysis for solutions described in the text (PDF). This material is available free of charge via the Internet at http://pubs.acs.org.

JA001545W

(60) The staggered configuration of the trimer is the lowest energy isomer. Therefore, it is reasonable to correlate the HOMO-LUMO gaps for the staggered trimers with the absorption edges on the long-wavelength side of the absorption bands assigned to trimers. This correlation is necessarily qualitative.

(61) Preisenberger, M.; Schier, A.; Schmidbaur, H. *J. Chem. Soc., Dalton Trans.* **1999**, 1645 and references therein.

(62) Omary, M. A.; Hall, D. R.; Shankle, G. E.; Siemiarczuck, A.; Patterson, H. H. *J. Phys. Chem. B* 1999, *103*, 3845.

(63) Rawashdeh-Omary, M. A.; Omary, M. A.; Patterson, H. H. *J. Phys. Chem. B* **2000**, *104*, 6143.